Food Chemistry 394 (2022) 133446

Contents lists available at ScienceDirect

Food Chemistry

journal homepage: www.elsevier.com/locate/foodchem

A ratio fluorescence sensor based on rhodamine B embedded metal-organic framework for glyphosate detection in agri-food products

Chao-Qun Wan [a], Yue-Hong Pang [a], Yong-Wei Feng [b], Xiao-Fang Shen [a,*]

[a] State Key Laboratory of Food Science and Technology, School of Food Science and Technology, Jiangnan University, Wuxi 214122, China
[b] Wuxi Institute for Food Control, Wuxi 214142, China

ARTICLE INFO

Keywords:
Glyphosate
Metal-organic framework
Ratio fluorescence sensor
Agri-food products
Rhodamine B

ABSTRACT

Glyphosate, a broad-spectrum and high-efficiency herbicide, could accumulate in the human body through the consumption of agri-food products. Herein, a ratio fluorescence sensor based on rhodamine B-embedded amino-functionalized iron-based metal-organic framework (MOF, NH_2-MIL-88(Fe)@RhB) bonded with Cu^{2+} was developed for rapid detection of glyphosate. The synthesized NH_2-MIL-88(Fe) was a biconical prism and had a cavity for the embedding of RhB as a reference compound. In the presence of Cu^{2+}, Lewis interactions with NH_2-MIL-88(Fe)@RhB cause the fluorescence signal to be turned off. When glyphosate was added, the signal was turned on due to chelation with Cu^{2+} and hydrogen bonding interactions with NH_2-MIL-88(Fe)@RhB. Under optimal conditions, the developed sensor exhibited a linear range of 0.60–45 μmol L^{-1} with a response time of less than 1 min. The sensor was applied in the analysis of agri-food products (tea, soybean, wheat, cucumber), with recoveries between 97.93% and 109.06%, indicating its promising application in agri-food safety.

1. Introduction

Glyphosate (N-[phosphonomethyl] glycine), a water-soluble, broad-spectrum, and high-efficiency herbicide, has been widely used for weed control in agricultural production fields since 1974 (Xu, Gu, Guo, Tong, & Chen, 2016; Duke, 2018). Glyphosate-resistant crops account for about 80% of all genetically modified crops, and the usage of glyphosate in the world has reached 825,800 tons per year (Nova, Calheiros, & Silva, 2020). Excessive glyphosate spraying in large areas has left residues in soil and surface water, which have shown to accumulate in human bodies through the food chain (Xu, Smith, Smith, Wang, & Li, 2019; Chang, Lin, Xiao, Chiu, & Hu, 2016). According to some authors, glyphosate is considered as an eco-friendly herbicide (Ighalo, Ajala, Adeniyi, Babatunde, & Ajala, 2021), and the carcinogenicity of glyphosate is inconclusive (Berry, 2020). However, doubts have arisen about its safety for human health, and several trials have already begun. Genotoxicity studies have revealed that pesticides, like glyphosate, non-specifically bind to the genetic material of vertebrates, thereby impacting the genetic integrity of native populations (Herek et al., 2021). Moreover, some studies suggested that glyphosate combined with surfactants may injure the vascular endothelium and restrict blood circulation (Kimura, Suzuki, Yokoyama, Kanetsuna, & Tanemoto, 2021). Therefore, it is of great importance to develop a rapid, reliable, and efficient analytical method for glyphosate in agri-food products.

The quantitative analysis of glyphosate is notoriously difficult, due to its low molecular weight and ionic character, high polarity, and good solubility in water as well as poor solubility in common organic solvents (Valle, Mello, Balvedi, Rodrigues, & Goulart, 2019). Conventional analysis methods have been applied to the detection of glyphosate, such as high-performance liquid chromatography (Li, Zhang, Kong, Qiao, & Xu, 2017), liquid chromatography-mass spectrometry (Ding et al., 2016), gas chromatography-flame photometric (Zhang et al., 2019), and ion chromatography (Dovidauskas, Okada, & dos Santos, 2020). Although these methods offer high sensitivity, they are not suitable for on-site detection as they require additional derivatization processes and tedious analysis. Fortunately, methods based on fluorometry or colorimetry are more rapid and convenient, thus satisfying this demand (Guan et al., 2021b). However, due to the absence of fluorophore or chromophore groups in glyphosate structures, an intermediate is needed to generate a quantitative signal. For example, anti-glyphosate antibody (Guan et al., 2021a) and tyrosinase (Hong, Ye, Dai, Wu, Chen, & Huang, 2020) have been used as intermediates for the fluorescence detection of glyphosate. To date, Cu^{2+}-based glyphosate fluorescence sensors have showcased promising applications. A coumarin derivative/Cu^{2+} sensing

* Corresponding author.
E-mail address: xfshen@jiangnan.edu.cn (X.-F. Shen).

https://doi.org/10.1016/j.foodchem.2022.133446
Received 28 December 2021; Received in revised form 6 June 2022; Accepted 7 June 2022
Available online 9 June 2022

system was developed, with a response time of 5 min and the R^2 of 0.990 (Wang et al., 2020). A turn-off fluorescence sensor based on the CuO/multiwall carbon nanotubes exhibited high selectivity for glyphosate, but it requires a 30 min response time (Chang et al., 2016). Typically, more than 5 min of response time is required in these Cu^{2+}-based detection methods, and the limitation of single emission makes the assay susceptible to the complex environment. Therefore, the development of a rapid glyphosate detection method with good stability is urgently needed.

Using a built-in reference, a series of stable fluorescent sources is incorporated into the sensor to correct the deviation caused by environmental influences and different equipment, thus improving the stability of the sensor. Several ratio probes with double-emission have been developed, such as a ratiometric dual lanthanide nanoprobe (Qu, Wang, & You, 2020) and double fluorescence quantum dots (Xu, Wei, Shi, Cai, Fu, & She, 2019). Moreover, recent studies have shown that the fluorescent characteristics of metal–organic frameworks (MOFs) could be used for sensors, and their unique cavities could provide a space for the embedding of reference molecules (Liao et al., 2018). Therefore MOFs went into sight as a kind of promising materials for fabricating ratio fluorescence sensors. For instance, an Eu^{3+}-based MOF was used for sensitive detection of tetracycline and L-tryptophan (Chen, Xu, Li, Xu, & Zhang, 2021; Li et al., 2021). A dual-emitting mixed-lanthanide MOF was constructed for ratio fluorescence sensing of Fe^{3+} and ascorbic acid (Yu et al., 2021).

In this work, we aimed to develop a MOF-based ratio fluorescence sensor for rapid glyphosate detection with high stability. More specifically, we developed a ratio fluorescence sensor based on NH_2-MIL-88(Fe)@RhB/Cu^{2+} for rapid glyphosate detection. Glyphosate directly enhanced the fluorescent signal of NH_2-MIL-88(Fe), thereby shortening the response time. Cu^{2+} was selected as an intermediate to enlarge the linear range, and the small molecule, RhB, was embedded into the NH_2-MIL-88(Fe) in order to correct the interference from the environment and equipment. The as-developed ratio fluorescence sensor offers a feasible platform for the practical analysis of agri-food products.

2. Experiment

2.1. Chemicals and reagents

All reagents were of analytical grade. Standard glyphosate was purchased from Aladdin Biochemical Technology Co., Ltd. (Shanghai, China). Rhodamine B and organic nitrogen- and phosphorous-based pesticides were purchased from Macklin Biochemical Technology Co., Ltd. (Shanghai, China). $FeCl_3$, 2-amino-1,4-benzene dicarboxylate (NH_2-BDC), dichloromethane, glacial acetic acid, and metal ions were obtained from Sinopharm Chemical Reagent Co., Ltd. (Shanghai, China). Ultrapure water was purchased from Wahaha Group Co., Ltd. (Hangzhou, China).

2.2. Instrumentation

All fluorescence spectra were collected via an F-7000 fluorescence spectrophotometer (Hitachi, Japan). The excitation and emission slit widths were 5 nm. The excitation wavelength was 382 nm. The morphology, structure, chemical groups, and elements of the materials were characterized by an SU8100 scanning electron microscope (SEM) (Hitachi, Japan). A D2 PHASER X-ray diffractometer (XRD) (Bruck AXS, Germany), an IS10 FT-IR spectrometer (Nicolet, USA), and Scientific K-Alpha X-ray photoelectron spectroscopy (XPS) (Thermo, USA), respectively.

2.3. Design of the NH_2-MIL-88(Fe)@RhB/Cu^{2+} ratio fluorescence sensor for glyphosate

The NH_2-MIL-88(Fe)@RhB was prepared from NH_2-BDC, $FeCl_3$, and RhB by the hydrothermal method (Fig. 1**A**). NH_2-BDC was chosen as the organic linker since amino-functionalized MOFs have been used for fluorescence detection of metal ions and organic substances with carboxyl groups. The dual-emitting fluorescence was constructed by embedding RhB into the cavity of NH_2-MIL-88(Fe) in order to eliminate the interference from the environment and equipment. Cu^{2+} was chosen as a quencher since Cu^{2+} as a common Lewis acid can accept electron pairs from the amino group, which acts as a Lewis base. Then, we applied NH_2-MIL-88(Fe)@RhB/Cu^{2+} for fluorescence detection of glyphosate from agri-foods (Fig. 1**B**). The strong chelation between Cu^{2+} and two oxygen atoms and one nitrogen atom from glyphosate created the competition in coordination with NH_2-MIL-88(Fe), thus generating a recovering of the fluorescence signal. Moreover, the hydrogen bonding interaction between the amino group from NH_2-MIL-88(Fe)@RhB and the carboxylic acid from glyphosate further enhanced the fluorescence signal. The fluorescent signal originating from RhB, a stable molecule, remained constant, and the ratio of the two distinct emission peaks was recorded as the analytical signal.

2.4. Synthesis of NH_2-MIL-88(Fe)@RhB

NH_2-MIL-88(Fe) was prepared according to a previous study, with some modifications (Zhang, Li, & Zhang, 2021). $FeCl_3$ (0.692 mmol) and NH_2-BDC (0.692 mmol) were added into 15 mL dimethylformamide solution of glacial acetic acid (3.50 mmol). After stirring at room temperature for 30 min, the mixture was transferred into a Teflon-lined steel autoclave and heated at 130 °C for 24 h. After cooling to room temperature, the mixture was centrifuged at 8000 r/min and washed with DMF/ethanol. The particles were collected and dried overnight under vacuum at 60 °C. The synthesis of NH_2-MIL-88(Fe)@RhB was similar to that of NH_2-MIL-88(Fe), except for the addition of RhB to the precursor solution, and the reaction time was correspondingly extended to 72 h.

2.5. Fluorescence response to Cu^{2+} and glyphosate

In a typical procedure, 2.5 mg NH_2-MIL-88(Fe)@RhB was added to 100 mL PBS buffer (pH 5.0, 0.1 mol L^{-1}), and a uniform dispersion solution was obtained after 20 min sonication. Afterwards, Cu^{2+} (0–60 μmol L^{-1}) or glyphosate (0–30 μmol L^{-1}) was added into the above solution, and the fluorescence intensity of NH_2-MIL-88(Fe)@RhB was recorded at an excitation wavelength of 382 nm.

2.6. Detection of glyphosate by NH_2-MIL-88(Fe)@RhB/Cu^{2+} sensor

The specific detection of glyphosate by NH_2-MIL-88(Fe)@RhB/Cu^{2+} was as follows: a solution of PBS buffer (0.1 mol L^{-1}, pH = 5.0) with NH_2-MIL-88(Fe)@RhB (2.5×10^{-2} g L^{-1}) and Cu^{2+} (50 μmol L^{-1}) was prepared. After stirring for 1 h, glyphosate (0–50 μmol L^{-1}) was added to the above solution. The fluorescence intensity was recorded with an excitation wavelength of 382 nm. Then, a standard curve for glyphosate was constructed, and the correlation coefficient was calculated. The limit of detection (LOD) was calculated using the mean fluorescence intensity of the blank control (in the absence of glyphosate) plus three times the value of the standard deviation.

In order to optimize the sensor, the pH of the sensor was changed using PBS buffer of pH 4–10. Different concentrations of NH_2-MIL-88(Fe)@RhB (0.5, 1.0, 2.5, 5.0, 7.5, and 10.0×10^{-2} g L^{-1}) were added to investigate the influence of NH_2-MIL-88(Fe)@RhB. The reaction time was optimized by detecting the fluorescence intensity in 5 min, and the interval time was 1 min. In these experiments, the ratio of the fluorescence intensity at 433 nm to that at 578 nm (I_{433}/I_{578}) before and after the addition of glyphosate was recorded, and the difference in I_{433}/I_{578} ($\triangle I_{433}/I_{578}$) was calculated for optimization.

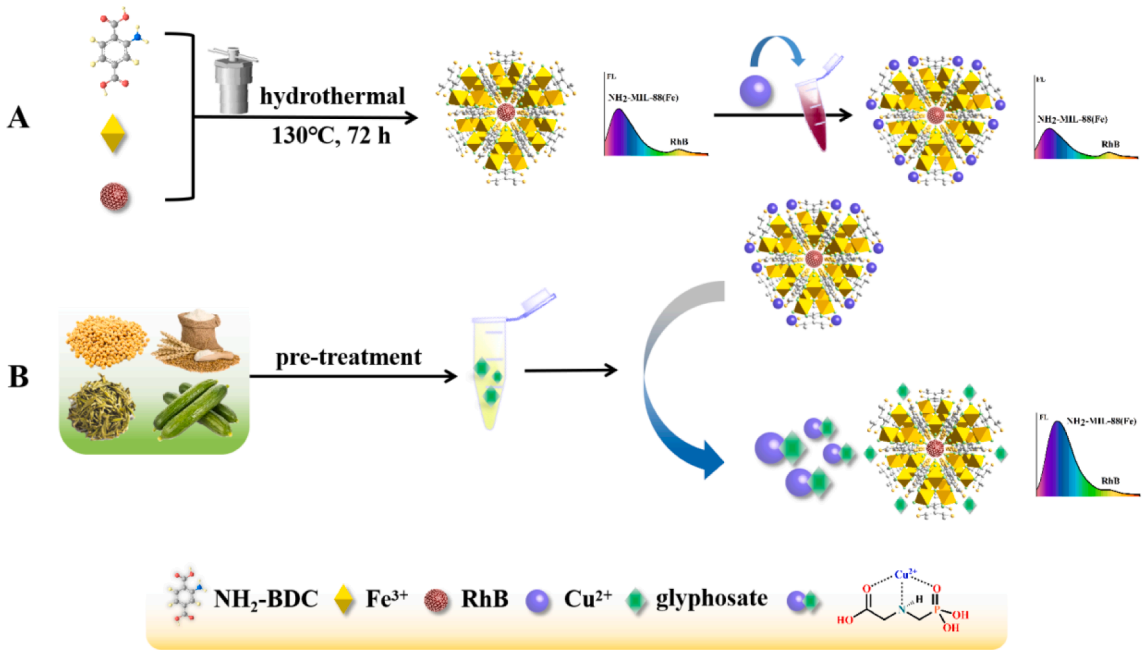

Fig. 1. Schematic diagram of (A) construction of NH_2-MIL-88(Fe)@RhB/Cu^{2+} ratio fluorescence sensor, and (B) application for detection of glyphosate.

2.7. Analysis of real samples

Agri-food products (tea, soybean, wheat, cucumber) were obtained from a local supermarket and stored at 4 °C before analysis. Dried samples (25 g) were extracted with 125 mL of distilled water for 30 min shaking. Then, the sample was centrifuged (10 min, 4500 r/min). For high-protein samples, such as soybean, 100 μL HCl was added, vortex-oscillated for 1 min, and centrifuged for 5 min. Then, 15 mL of the supernatant was extracted with 15 mL dichloromethane by vortexing for 2 min followed by centrifugation for 5 min. Finally, the pH of the extract was adjusted with PBS buffer (pH 5.0, 0.1 mol L^{-1}). The mixture was subsequently filtered through a 0.45-μm membrane for glyphosate detection. Different concentrations (5 and 10 μmol L^{-1}) of glyphosate standard solutions were added into these four samples and were detected by the proposed method. Each sample was measured five times.

3. Results and discussion

3.1. Characterizations of NH_2-MIL-88(Fe)@RhB

The prepared NH_2-MIL-88(Fe) particles (Fig. 2**A**), as indicated in the SEM images, have biconical prism structures with about 500 nm elongation of the octahedra, which is similar to previous reports (Asmar, Baalbaki, Khalil, Naim, Bejjani, & Ghauch, 2021). In addition, the morphology of NH_2-MIL-88(Fe)@RhB (Fig. 2**B**) was similar to that of NH_2-MIL-88(Fe), indicating that the introduction of the RhB molecule did not influence the lattice structure of NH_2-MIL-88(Fe). The XRD diffraction peaks of NH_2-MIL-88(Fe)@RhB (Fig. 2**C**) show that the crystal structure changed very little after doping with RhB. The crystal structure was well-defined and had the same diffraction peaks as the simulated NH_2-MIL-88(Fe) (Liédana, Lozano, Galve, Téllez, & Coronas, 2014).

The XPS spectrum of NH_2-MIL-88(Fe)@RhB (Fig. 2**D**) shows peaks located at 284.0, 399.3, 531.1, and 711.1 eV, which were ascribed to C 1 s, N 1 s, O 1 s, and Fe 2p, respectively. These peaks prove the existence of Fe atoms and N atoms in the composite. The spectrum of Fe 2p (Fig. 2**E**) contained two peaks, relating to Fe $2p_{3/2}$ (711.0 eV) and Fe $2p_{1/2}$ (724.4 eV), corresponding to the binding energy of Fe (III). In the case of N 1 s (Fig. 2**F**), the peaks centered at 399.3 eV and 401.5 eV were ascribed to the C—N/N—H and N–C═O of the amino groups from the NH_2-BDC (Zhao et al., 2020).

3.2. Fluorescence response and possible mechanism of NH_2-MIL-88(Fe)@RhB

The fluorescence spectrum of NH_2-MIL-88(Fe)@RhB exhibited two distinct emission peaks located at 433 nm and 578 nm, originating from NH_2-MIL-88(Fe) and RhB, respectively (**Fig. S1**). First, we tested the quenching of the NH_2-MIL-88(Fe)@RhB by Cu^{2+}. The fluorescence at 433 nm was gradually quenched with the addition of Cu^{2+}, and this was likely due to the interaction of Cu^{2+} with amino groups exposed on the surface of the nanocomposite (Duan & Huang, 2017). The quenching effect of NH_2-MIL-88(Fe)@RhB was linearly correlated with the concentration of Cu^{2+}. Moreover, the emission intensity at 578 nm for RhB was not significantly affected, which suggests that our strategy of the ratio fluorescence sensor is viable and accurate.

Next, we investigated the change in fluorescence due to the interaction of glyphosate with NH_2-MIL-88(Fe)@RhB. An increase in the fluorescence intensity at 433 nm and a 15-nm red shift were observed after adding glyphosate (**Fig. S2**). This enhancement is mainly due to the hydrogen bonding interactions between the amino group from NH_2-MIL-88(Fe)@RhB and the carboxylic acid from glyphosate. Most reported fluorescence probes are based on the quenching effect of Cu^{2+} to detect glyphosate. Our developed NH_2-MIL-88(Fe)@RhB probe directly enhanced the fluorescence signals by glyphosate. In addition, the characteristic emission of the RhB remained nearly unchanged. The fluorescence enhancement effect of NH_2-MIL-88(Fe)@RhB was linearly correlated with the concentration of glyphosate, indicating that the fluorescence sensor based on NH_2-MIL-88(Fe)@RhB is a promising candidate for glyphosate analysis.

Based on the "on-off" sensing strategy mediated by Cu^{2+} and the enhancement mechanism directly induced by glyphosate, we developed the NH_2-MIL-88(Fe)@RhB/Cu^{2+} fluorescence sensor. Digital photos under UV light at 365 nm (Fig. 3**A**) show that the fluorescence was quenched by adding Cu^{2+} and then was enhanced by adding glyphosate. Consistent with the digital photos, the addition of 50 μmol L^{-1} Cu^{2+} produced a 37% quenching effect. After adding 45 μmol L^{-1} glyphosate, the fluorescence was enhanced by 192%. Furthermore, the fluorescence

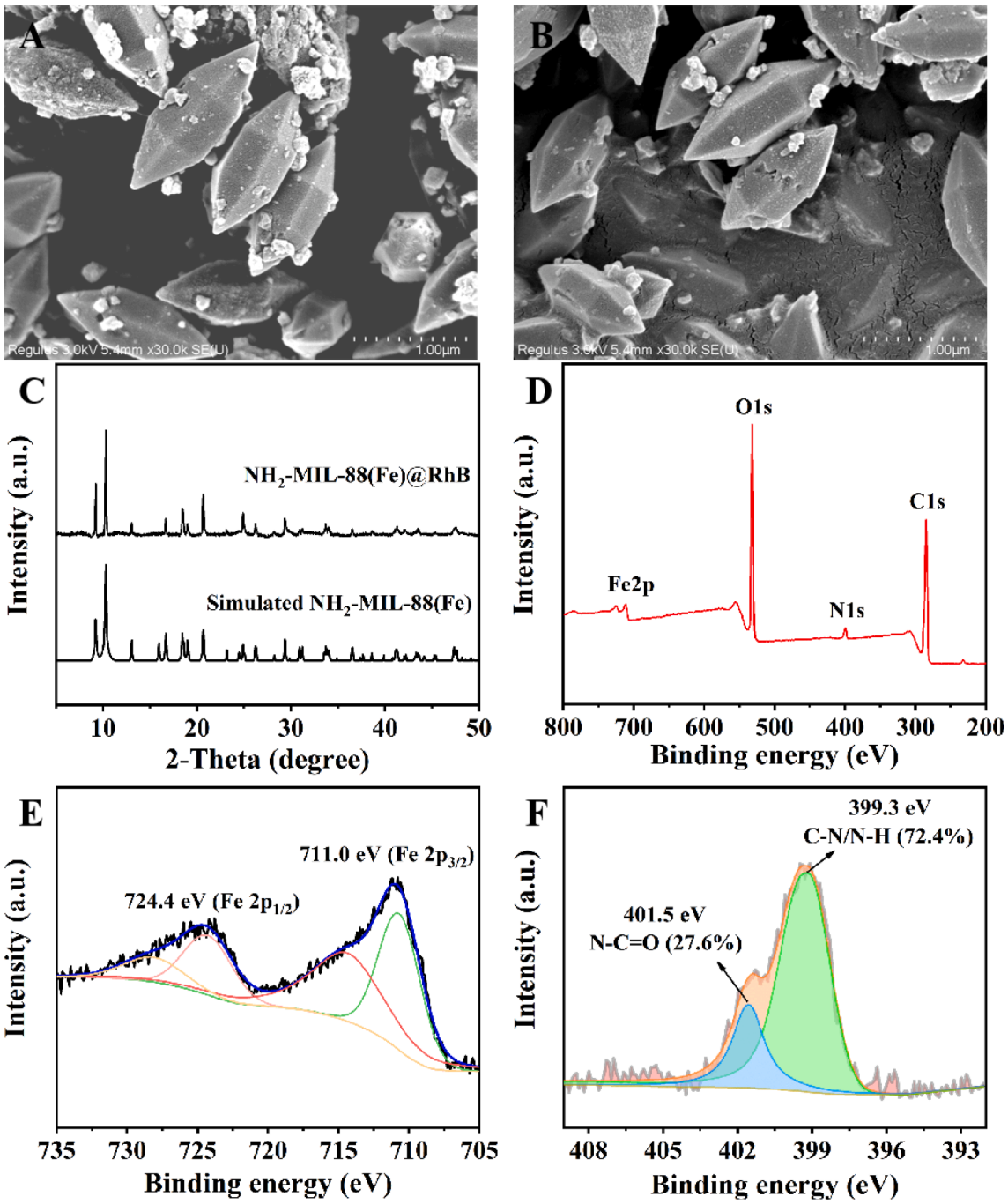

Fig. 2. SEM images of the synthesized (A) NH_2-MIL-88(Fe) and (B) NH_2-MIL-88(Fe)@RhB. (C) XRD patterns of the simulated NH_2-MIL-88(Fe) and the synthesized NH_2-MIL-88(Fe)@RhB. (D) XPS survey spectra of NH_2-MIL-88(Fe)@RhB. Narrow scan spectra of (E) Fe 2p and (F) N 1 s.

intensity at 578 nm was not significantly affected by Cu^{2+} or glyphosate.

To explain the above experimental results, the FT-IR spectra of NH_2-MIL-88(Fe)@RhB before and after the addition of Cu^{2+} were recorded (Fig. 3**B**). In the FT-IR spectrum of NH_2-MIL-88(Fe)@RhB, the characteristic peak at 3416 cm^{-1} was attributed to the stretching vibration of the –OH group. The peaks at 1652 and 855 cm^{-1} were assigned to the deformation vibrations of N—H and the peak at 523 cm^{-1} was attributed to Fe. Remarkably, the peaks assigned to the amino group in NH_2-MIL-88(Fe)@RhB disappeared after adding Cu^{2+}, which confirmed the combination of Cu^{2+} and –NH_2, which were exposed on the NH_2-MIL-88 (Fe)@RhB (**Fig. S3**).

Based on our experimental results and a previous study (Guan et al., 2021b), the existence of glyphosate could increase the fluorescence on account of the strong chelation between Cu^{2+} and two oxygen atoms and one nitrogen atom from glyphosate, leading to the competition in coordination with NH_2-MIL-88(Fe) (**Fig. S3**). To verify this assumption, the Cu 2p narrow scan XPS spectra of NH_2-MIL-88(Fe)@RhB/Cu^{2+} before (Fig. 3**C**) and after (Fig. 3**D**) the addition of glyphosate were investigated. The peak at 952.2 eV, assigned to Cu $2p_{1/2}$, was shifted to 952.7 eV in the presence of glyphosate, which demonstrates the stronger bonding capacity of glyphosate with Cu^{2+}, compared to the NH_2-MIL-88 (Fe).

The N 1 s narrow scan XPS spectra of NH_2-MIL-88(Fe)@RhB/Cu^{2+} before (Fig. 3**E**) and after (Fig. 3**F**) the addition of glyphosate were also recorded. The N 1 s spectrum can be fitted into two peaks, representing C—N/N—H and N–C═O, respectively (Zhang et al., 2021). Comparing

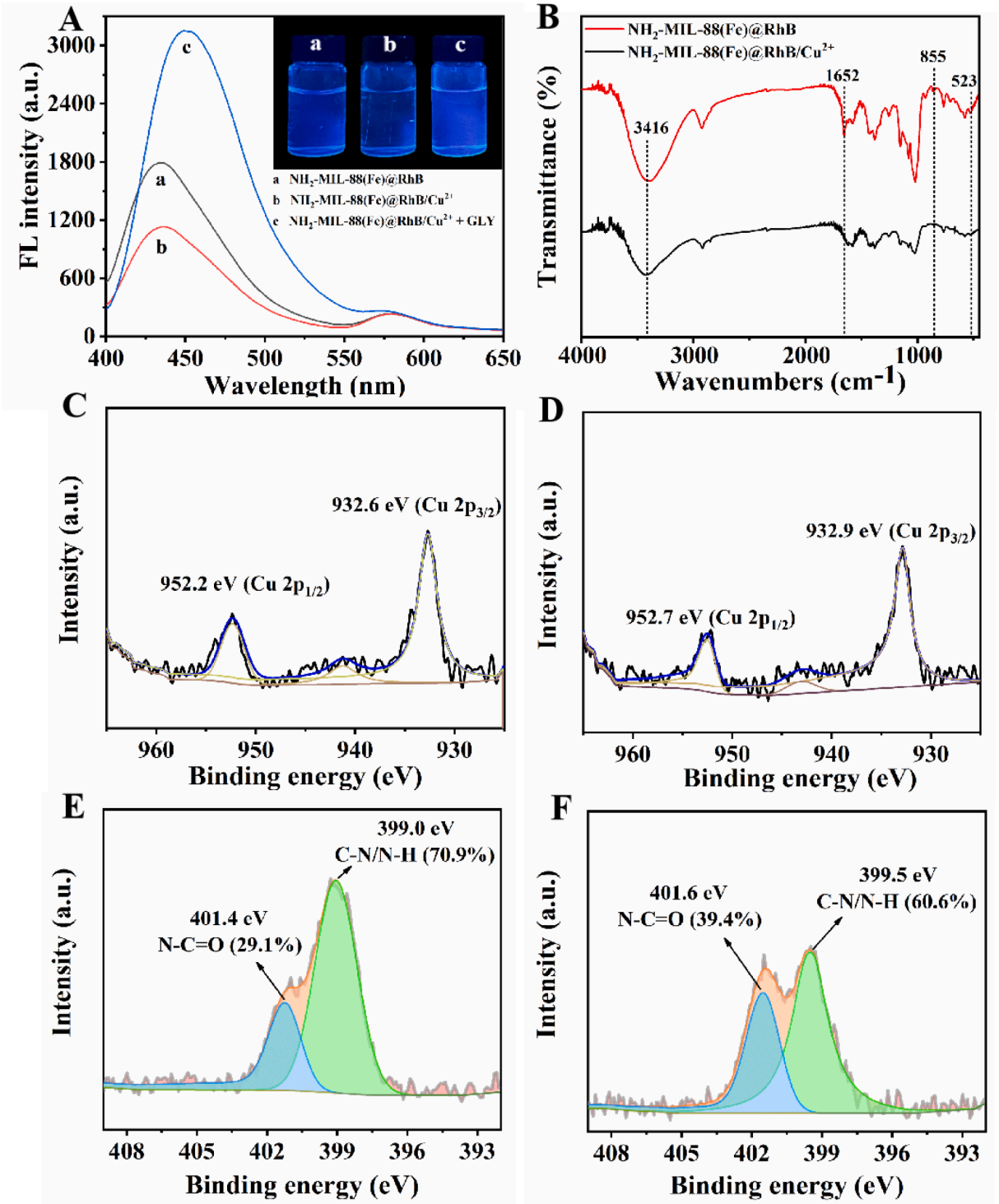

Fig. 3. (A) Fluorescence spectra of NH_2-MIL-88(Fe)@RhB (curve a), NH_2-MIL-88(Fe)@RhB/Cu^{2+} (curve b), and NH_2-MIL-88(Fe)@RhB/Cu^{2+} + GLY (curve c, glyphosate 45 μmol L^{-1}). Inset: Digital photos under UV light at 365 nm. (B) The FT-IR spectra of NH_2-MIL-88(Fe)@RhB with and without Cu^{2+}. The Cu 2p (C) and N1s (E) narrow scan XPS spectra of NH_2-MIL-88(Fe)@RhB/Cu^{2+}, and the Cu 2p (D) and N1s (F) narrow scan XPS spectra of NH_2-MIL-88(Fe)@RhB/Cu^{2+} after adding glyphosate.

the spectrum before and after adding Cu^{2+}, the content of C—N/N—H dropped from 72.4% to 70.9%, suggesting that the Cu^{2+} interfered with the amino groups exposed on the NH_2-MIL-88(Fe)@RhB, and this result is in accordance with the results of FT-IR analysis. However, with the addition of glyphosate to NH_2-MIL-88(Fe)@RhB/Cu^{2+}, the content of N–C═O increased from 29.1% to 39.4%, corresponding to hydrogen bonding interactions between the amino groups with lone pair electrons exposed on NH_2-MIL-88(Fe)@RhB and the carboxylic acid from glyphosate (Fig. S3).

3.3. Optimization of conditions for glyphosate detection

Glyphosate contains carboxylic acid groups, which are deprotonated in alkaline conditions, therefore, pH always influences the sensitivity of

glyphosate detection (Wang, Liu, Yuan, & Ma, 2016). Thus, the ratio of the fluorescence intensity of NH_2-MIL-88(Fe)@RhB/Cu^{2+} at 433 nm to that at 578 nm (I_{433}/I_{578}) in the pH range of 4.0–10.0 was investigated (Fig. 4**A**). When the pH increased from 4.0 to 5.0, the difference in I_{433}/I_{578} ($\triangle I_{433}/I_{578}$) increased to 4.1 and remained stable in the range of 5.0–7.0. When the pH was higher than 7.0, $\triangle I_{433}/I_{578}$ decreased. The maximum I_{433}/I_{578} was obtained at pH 5.0, thus, the following experiments were performed at pH 5.0.

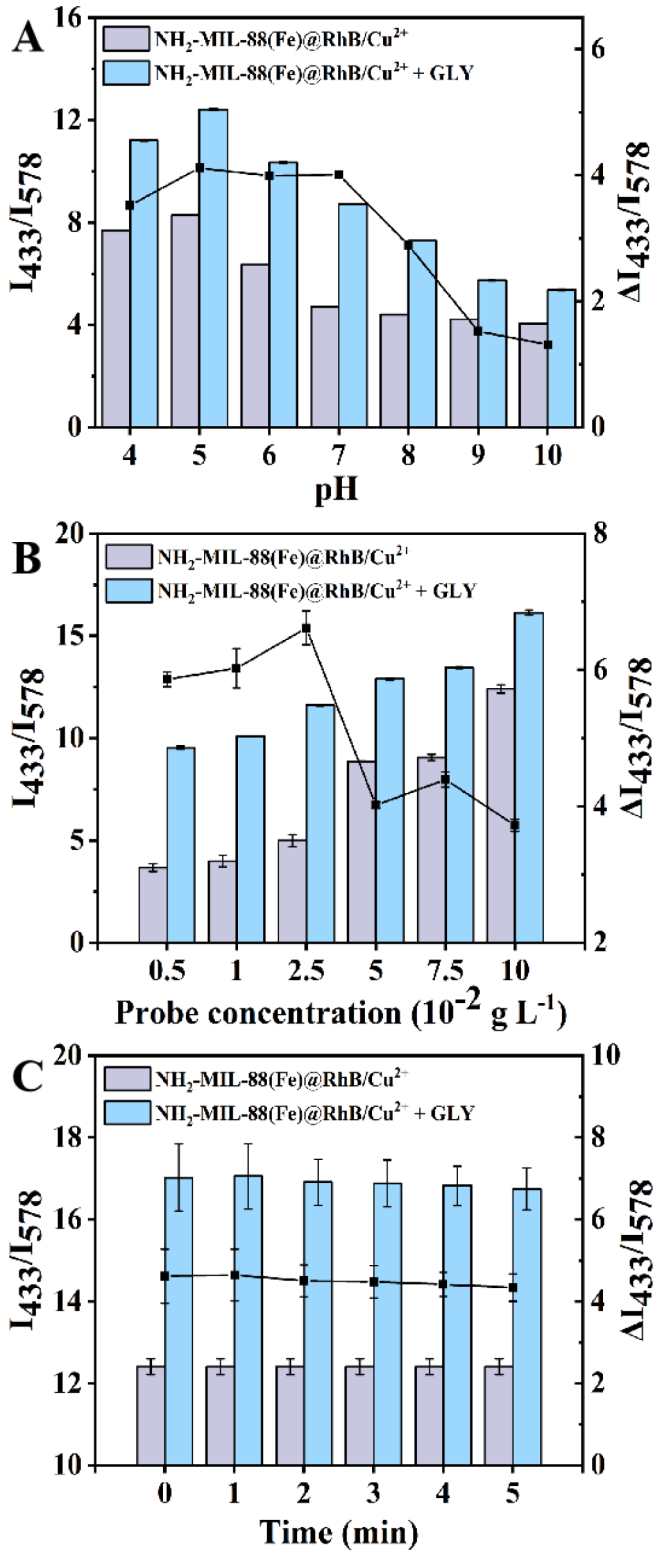

Fig. 4. Ratio of NH_2-MIL-88(Fe)@RhB fluorescence intensity at 433 nm to 578 nm with different (A) pH values of the system, (B) probe concentrations, and (C) time. The illustrated error bars represent the standard deviation of three repetitive measurements.

The concentration of the probe directly affected the intensity of the fluorescence, thus affecting the sensitivity and precision of the sensor. The I_{433}/I_{578} of NH_2-MIL-88(Fe)@RhB/Cu^{2+} upon the concentration of NH_2-MIL-88(Fe)@RhB at 0.5, 1.0, 2.5, 5.0, 7.5, 10.0 was investigated (Fig. 4**B**). As the concentration of NH_2-MIL-88(Fe)@RhB increased, an increasing trend in I_{433}/I_{578} was observed. The maximum $\triangle I_{433}/I_{578}$ was obtained at 2.5×10^{-2} g L^{-1} (6.6), but when the concentration of NH_2-MIL-88(Fe)@RhB was over 2.5×10^{-2} g L^{-1}, the value of $\triangle I_{433}/I_{578}$ declined to 4.0. Thus, the interaction between glyphosate and NH_2-MIL-88(Fe)@RhB /Cu^{2+} was more prominent at 2.5×10^{-2} g L^{-1}.

To assess the influence of the reaction time on the fluorescence intensity of NH_2-MIL-88(Fe)@RhB/Cu^{2+}, we observed the change in I_{433}/I_{578} over 5 min (Fig. 4**C**). No substantial differences in the ratio enhancement were observed. To be consistent, 1 min was chosen as the reaction time for the following studies.

3.4. Method validation

To evaluate the reliability and efficiency of the optimized method, we subsequently investigated the detection of glyphosate. As shown in Fig. 5**A**, with increasing glyphosate concentration, the fluorescence intensity increased significantly at 433 nm in conjunction with a 15-nm red shift. Simultaneously, the fluorescence intensity of RhB showed very little change during the experiments. The fluorescence ratio of I_{433}/I_{578} shows a good linearity for glyphosate at 0.6–15 μmol L^{-1} (R^2 = 0.9977) and 15–45 μmol L^{-1} (R^2 = 0.9987) (Fig. 5**B**), and in the linearity at the concentration of 0.6–15 μmol L^{-1}, the sensor had a good sensitivity ($I_{433}/I_{578} = 0.2681X + 6.3939$). The LOD for glyphosate was 0.18 μmol L^{-1}.

Moreover, we estimated the selectivity of the sensor for glyphosate (25 μmol L^{-1}), compared to other organic nitrogen- and phosphorous-based pesticides (chlorpyrifos, paclobutrazol, thimet, parathion, parathion-methyl, fenthion, phosalone, phoxim, 2.5 mmol L^{-1}) (Fig. 5**C**). As expected, there was no significant enhancement of the ratio in I_{433}/I_{578}, except for the addition of glyphosate, and this indicates high selectivity of the sensor. The selectivity of the sensor for glyphosate (25 μmol L^{-1}), compared with other pesticides (chlorpyrifos, paclobutrazol, thimet, parathion, parathion-methyl, fenthion, phosalone, phoxim, 2.5 mmol L^{-1}), was further analyzed (Fig. 5**D**). Even in the presence of these similar-structured pesticides, the NH_2-MIL-88(Fe)@RhB still showed a 200% fluorescent enhancement from glyphosate, further confirming the high selectivity of the sensor.

In Table S1, we compare our sensor with other methods for glyphosate detection found in the literature. The sensor presented here has the notable advantage of short response time (less than 1 min). Moreover, we embedded RhB into the cavity of the NH_2-MIL-88(Fe) to eliminate the interference from the environment and equipment and enhance the stability of the sensor. The sensitivity and accuracy of the sensor are also satisfactory, demonstrating its potential application for on-site detection of glyphosate for food safety.

3.5. Application in real samples

The applicability and reliability of the proposed method were further assessed by determining glyphosate in four agri-food products (tea, soybean, wheat, cucumber). The average of five measurements is shown in Table 1 and **Fig. S5**. Glyphosate was found in soybean at 5.26 μmol L^{-1}. The recovery of glyphosate was 97.93%–109.06% (RSD < 8.4%), indicating that the developed ratio fluorescence sensor is a reliable platform for quantitative detection of glyphosate in agri-food products.

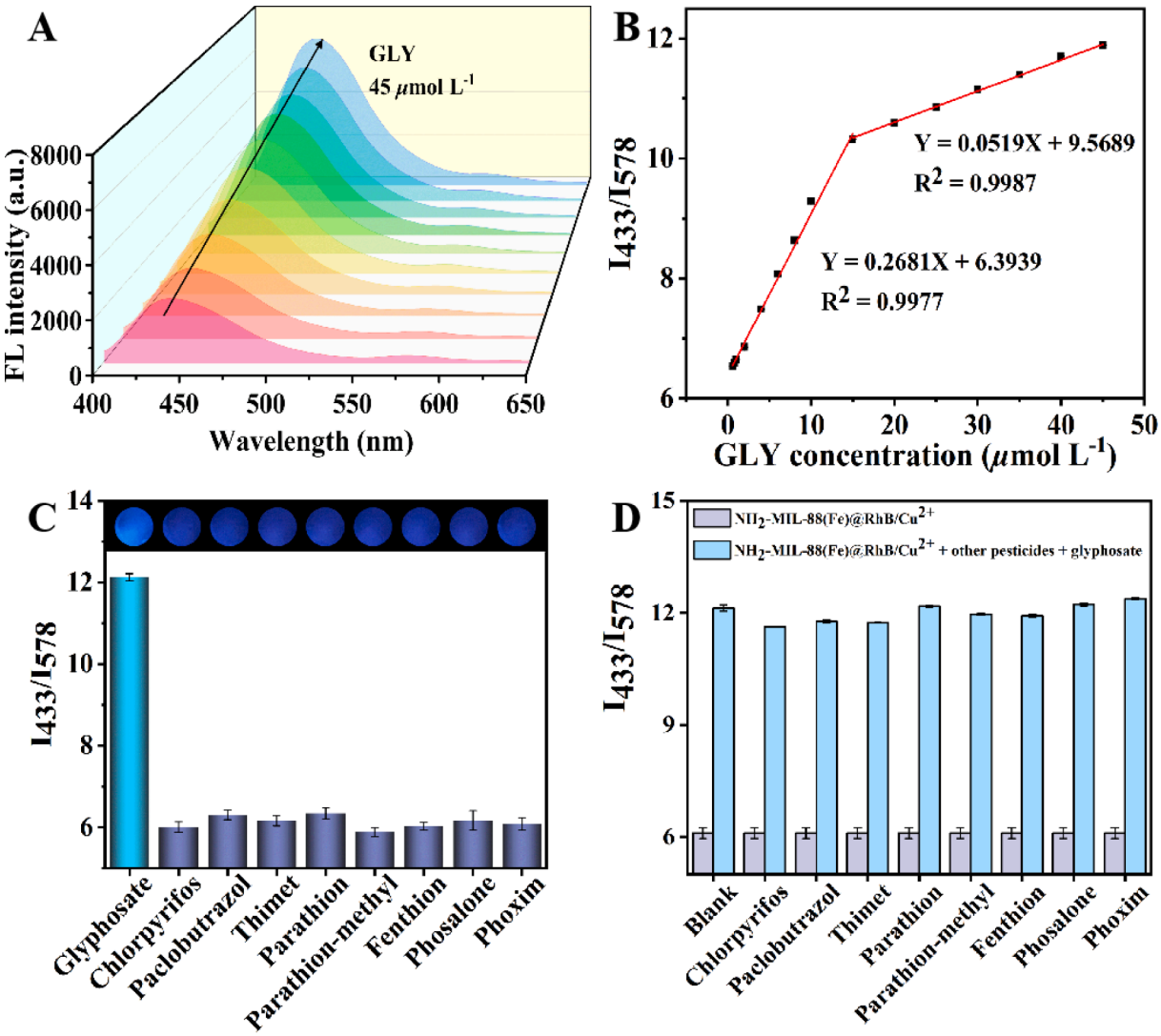

Fig. 5. (A) Fluorescence spectra of NH_2-MIL-88(Fe)@RhB/Cu^{2+} (2.5×10^{-2} g L^{-1}) in PBS buffer (0.1 mol L^{-1}, pH = 5.0) upon gradual addition of glyphosate (0–45 μmol L^{-1}). (B) The linear range of glyphosate. (C) Selectivity of NH_2-MIL-88(Fe)@RhB/Cu^{2+} (2.5×10^{-2} g L^{-1}) to glyphosate (25 μmol L^{-1}) and other pesticides (2.5 mmol L^{-1}). Insets: Digital photos under UV light at 365 nm. (D) Ratio changes of fluorescence intensity between 433 nm and 578 nm by glyphosate (25 μmol L^{-1}) in the absence and presence of other pesticides (2.5 mmol L^{-1}).

Table 1
Detection of glyphosate in agri-food products.

Samples	Added (μmol L^{-1})	Found (μmol L^{-1})	Recovery (%)	RSD (n = 5) (%)
Tea	0	ND[1]	—	—
	5	5.30	105.93	5.8
	10	10.91	109.06	8.4
Cucumber	0	ND	—	—
	5	5.31	106.15	1.7
	10	10.23	102.33	1.9
Soybean	0	5.26	—	3.1
	5	9.90	97.93	4.5
	10	14.85	98.49	2.4
Wheat	0	ND	—	—
	5	5.29	105.80	1.6
	10	9.90	98.95	0.9

ND[1]: Not detected.

4. Conclusion

In summary, we developed a rapid ratio fluorescence sensor based on NH_2-MIL-88(Fe)@RhB–Cu^{2+} bonding to analyze glyphosate in agri-food products (tea, soybean, wheat, cucumber). The embedding of RhB into the cavity of the NH_2-MIL-88(Fe) eliminated the interference from the environment and the equipment, resulting in enhanced stability of the sensor. Moreover, our developed method has the advantages of a short response time, and reveals a good performance with high selectivity for glyphosate. Due to the fast response and visible fluorescence of the material, NH_2-MIL-88(Fe)@RhB/Cu^{2+} provides an efficient detection method for glyphosate, with great potential as an on-site detection sensor for food safety.

CRediT authorship contribution statement

Chao-Qun Wan: Conceptualization, Methodology, Formal analysis, Investigation, Writing – original draft. **Yue-Hong Pang:** Methodology, Formal analysis, Validation, Investigation, Funding acquisition. **Yong-Wei Feng:** Conceptualization, Methodology, Investigation. **Xiao-Fang Shen:** Conceptualization, Resources, Writing – review & editing, Project administration, Funding acquisition.

Declaration of Competing Interest

The authors declare that they have no known competing financial interests or personal relationships that could have appeared to influence the work reported in this paper.

Data availability

The authors are unable or have chosen not to specify which data has been used.

Acknowledgements

This work was supported by the National Natural Science Foundation of China (22076067, 21976070).

Appendix A. Supplementary data

Supplementary data to this article can be found online at https://doi.org/10.1016/j.foodchem.2022.133446.

References

Berry, C. (2020). Glyphosate and cancer: The importance of the whole picture. *Pest Management Science, 76*(9), 2874–2877. https://doi.org/10.1002/ps.5834

Chang, Y. C., Lin, Y. S., Xiao, G. T., Chiu, T. C., & Hu, C. C. (2016). A highly selective and sensitive nanosensor for the detection of glyphosate. *Talanta, 161*, 94–98. https://doi.org/10.1016/j.talanta.2016.08.029

Chen, J., Xu, Y., Li, S., Xu, F., & Zhang, Q. (2021). Ratio fluorescence detection of tetracycline by a Eu^{3+}/NH_2-MIL-53(Al) composite. *RSC Advances, 11*(4), 2397–2404. https://doi.org/10.1039/D0RA09185E

Ding, J., Jin, G., Jin, G., Shen, A., Guo, Z., Yu, B., & Liang, X. (2016). Determination of Underivatized Glyphosate Residues in Plant-Derived Food with Low Matrix Effect by Solid Phase Extraction-Liquid Chromatography-Tandem Mass Spectrometry. *Food Analytical Methods, 9*(10), 2856–2863. https://doi.org/10.1007/s12161-016-0468-8

Dovidauskas, S., Okada, I. A., & dos Santos, F. R. (2020). Validation of a simple ion chromatography method for simultaneous determination of glyphosate, aminomethylphosphonic acid and ions of Public Health concern in water intended for human consumption. *Journal of Chromatography A, 1632*, Article 461603. https://doi.org/10.1016/j.chroma.2020.461603

Duan, S., & Huang, Y. (2017). Electrochemical sensor using NH_2-MIL-88(Fe)-rGO composite for trace Cd^{2+}, Pb^{2+}, and Cu^{2+} detection. *Journal of Electroanalytical Chemistry, 807*, 253–260. https://doi.org/10.1016/j.jelechem.2017.11.051

Duke, S. O. (2018). The history and current status of glyphosate. *Pest Management Science, 74*(5), 1027–1034. https://doi.org/10.1002/ps.4652

El Asmar, R., Baalbaki, A., Abou Khalil, Z., Naim, S., Bejjani, A., & Ghauch, A. (2021). Iron-based metal organic framework MIL-88-A for the degradation of naproxen in water through persulfate activation. *Chemical Engineering Journal, 405*, Article 126701. https://doi.org/10.1016/j.cej.2020.126701

Guan, J., Yang, J., Zhang, Y., Zhang, X., Deng, H., Xu, J., & Yuan, M. S. (2021). Employing a fluorescent and colorimetric picolyl-functionalized rhodamine for the detection of glyphosate pesticide. *Talanta, 224*, Article 121834. https://doi.org/10.1016/j.talanta.2020.121834

Guan, N., Li, Y., Yang, H., Hu, P., Lu, S., Ren, H., & Zhou, Y. (2021). Dual-functionalized gold nanoparticles probe based bio-barcode immuno-PCR for the detection of glyphosate. *Food Chemistry, 338*, Article 128133. https://doi.org/10.1016/j.foodchem.2020.128133

Herek, J. S., Vargas, L., Rinas Trindade, S. A., Rutkoski, C. F., Macagnan, N., Hartmann, P. A., & Hartmann, M. T. (2021). Genotoxic effects of glyphosate on Physalaemus tadpoles. *Environmental Toxicology and Pharmacology, 81*, Article 103516. https://doi.org/10.1016/j.etap.2020.103516

Hong, C., Ye, S., Dai, C., Wu, C., Chen, L., & Huang, Z. (2020). Sensitive and on-site detection of glyphosate based on papain-stabilized fluorescent gold nanoclusters. *Analytical and Bioanalytical Chemistry, 412*(29), 8177–8184. https://doi.org/10.1007/s00216-020-02952-7

Ighalo, J. O., Ajala, O. J., Adeniyi, A. G., Babatunde, E. O., & Ajala, M. A. (2021). Ecotoxicology of glyphosate and recent advances in its mitigation by adsorption. *Environmental Science and Pollution Research, 28*(3), 2655–2668. https://doi.org/10.1007/s11356-020-11521-5

Kimura, T., Suzuki, M., Yokoyama, T., Kanetsuna, Y., & Tanemoto, M. (2021). Lessons for the clinical nephrologist: Acute kidney injury by a glyphosate-surfactant herbicide. *Journal of Nephrology*. https://doi.org/10.1007/s40620-021-00975-6

Li, D., Zhang, X., Kong, F., Qiao, X., & Xu, Z. (2017). Molecularly Imprinted Solid-Phase Extraction Coupled with High-Performance Liquid Chromatography for the Determination of Trace Trichlorfon and Monocrotophos Residues in Fruits. *Food Analytical Methods, 10*(5), 1284–1292. https://doi.org/10.1007/s12161-016-0687-z

Li, Y., Gao, G., Wu, S., Zhang, Y., Fedin, V., Zhu, M. C., & Gao, E. (2021). An Eu-based MOF as fluorescent probe for the sensitive detection of L-tryptophan. *Journal of Solid State Chemistry, 304*. https://doi.org/10.1016/j.jssc.2021.122555

Liao, W. M., Zhang, J. H., Yin, S. Y., Lin, H., Zhang, X., Wang, J., & Su, C. Y. (2018). Tailoring exciton and excimer emission in an exfoliated ultrathin 2D metal-organic framework. *Nature Communications, 9*(1), 2401. https://doi.org/10.1038/s41467-018-04833-1

Liédana, N., Lozano, P., Galve, A., Téllez, C., & Coronas, J. (2014). The template role of caffeine in its one-step encapsulation in MOF NH_2-MIL-88B(Fe). *Journal of Materials Chemistry B, 2*(9), 1144–1151. https://doi.org/10.1039/C3TB21707H

Nova, P., Calheiros, C. S. C., & Silva, M. (2020). Glyphosate in Portuguese Adults - A Pilot Study. *Environmental Toxicology and Pharmacology, 80*. https://doi.org/10.1016/j.etap.2020.103462

Qu, F., Wang, H., & You, J. (2020). Dual lanthanide-probe based on coordination polymer networks for ratiometric detection of glyphosate in food samples. *Food Chemistry, 323*, Article 126815. https://doi.org/10.1016/j.foodchem.2020.126815

Valle, A. L., Mello, F. C. C., Alves-Balvedi, R. P., Rodrigues, L. P., & Goulart, L. R. (2019). Glyphosate detection: Methods, needs and challenges. *Environmental Chemistry Letters, 17*(1), 291–317. https://doi.org/10.1007/s10311-018-0789-5

Wang, S., Liu, B., Yuan, D., & Ma, J. (2016). A simple method for the determination of glyphosate and aminomethylphosphonic acid in seawater matrix with high performance liquid chromatography and fluorescence detection. *Talanta, 161*, 700–706. https://doi.org/10.1016/j.talanta.2016.09.023

Wang, X., Sakinati, M., Yang, Y., Ma, Y., Yang, M., Luo, H., & Huo, D. (2020). The construction of a CND/Cu^{2+} fluorescence sensing system for the ultrasensitive detection of glyphosate. *Analytical Methods, 12*(4), 520–527. https://doi.org/10.1039/C9AY02303H

Xu, J., Gu, X., Guo, Y., Tong, F., & Chen, L. (2016). Adsorption behavior and mechanism of glufosinate onto goethite. *Science of The Total Environment, 560–561*, 123–130. https://doi.org/10.1016/j.scitotenv.2016.03.239

Xu, J., Smith, S., Smith, G., Wang, W., & Li, Y. (2019). Glyphosate contamination in grains and foods: An overview. *Food Control, 106*, Article 106710. https://doi.org/10.1016/j.foodcont.2019.106710

Xu, L., Wei, L., Shi, Q., Cai, C., Fu, H. Y., & She, Y. B. (2019). Non-targeted Detection of Multiple Frauds in Orange Juice Using Double Water-Soluble Fluorescence Quantum Dots and Chemometrics. *Food Analytical Methods, 12*(11), 2614–2622. https://doi.org/10.1007/s12161-019-01570-z

Yu, H., Liu, Q., Li, J., Su, Z. M., Li, X., Wang, X., & Hu, X. (2021). A dual-emitting mixed-lanthanide MOF with high water-stability for ratiometric fluorescence sensing of Fe^{3+} and ascorbic acid. *Journal of Materials Chemistry C, 9*(2), 562–568. https://doi.org/10.1039/D0TC04781C

Zhang, W., Feng, Y., Ma, L., An, J., Zhang, H., Cao, M., & Lian, K. (2019). A method for determining glyphosate and its metabolite aminomethyl phosphonic acid by gas chromatography-flame photometric detection. *Journal of Chromatography A, 1589*, 116–121. https://doi.org/10.1016/j.chroma.2018.12.039

Zhang, Y., Li, Y., & Zhang, L. (2021). Fabricating multifunctional low-toxicity ratiometric fluorescent probe for individual detection of Cu^{2+}/glutamate and continuous sensing for glutamate via Cu^{2+}-based platform. *Spectrochimica Acta Part A: Molecular and Biomolecular Spectroscopy, 259*, Article 119892. https://doi.org/10.1016/j.saa.2021.119892

Zhao, F., Su, C., Yang, W., Han, Y., Luo, X., Li, C., & Li, Z. (2020). In-situ growth of UiO-66-NH_2 onto polyacrylamide-grafted nonwoven fabric for highly efficient Pb(II) removal. *Applied Surface Science, 527*, Article 146862. https://doi.org/10.1016/j.apsusc.2020.146862